

Origin of Convoy Electrons Produced by Swift Neutral Hydrogen and Proton Beams Traversing Carbon Foils

Y. Yamazaki and N. Oda

*Research Laboratory for Nuclear Reactors, Tokyo Institute of Technology,
Ookayama, Meguro-ku, Tokyo 152, Japan*

(Received 16 September 1983)

An experiment is presented demonstrating that for both swift neutral hydrogen and proton bombardments (0.9–2.0 MeV/u) on carbon foils, the origin of cusp-shaped convoy electrons is mainly attributable to a final-state interaction between projectiles and free secondary electrons traveling with velocities around the projectile velocities near the exit surface of the target foils. The direct contribution to the cusp-shaped convoy electrons of target-electron transfer to the projectile continuum is found to be relatively unimportant.

PACS numbers: 34.50.Hc, 79.20.Nc

In ion-solid-foil collisions, a sharp peak in the energy spectrum of electrons is observed in the forward directions at the velocity of the emerging ions, and the electrons in the peak are usually called "convoy electrons." During the last decade, the origin of the convoy electrons has been investigated with increasing interest.¹ Several production mechanisms of the convoy electrons have been proposed, such as target-electron transfer to the projectile continuum (hereafter referred to as TETC),² projectile-electron loss to the projectile continuum (ELC),³ and wake-riding electron release to the projectile continuum (WRC).⁴ Experimentally, the shapes and intensities of convoy-electron spectra as functions of projectile species, projectile energy, and electron ejection angle have so far been observed for foil targets thick enough to attain "equilibrium spectra."⁵ The linear proportionality of the convoy peak width to the projectile velocity has been most intensively investigated to test the validity of the TETC process.⁶ However, it is worth pointing out that such a linear proportionality relation is not specific to the TETC mechanism but is expected to hold generally for processes where low-lying, projectile-centered isotropic continuum states are concerned as final states.

Recently, new aspects of convoy electrons have been reported: (i) Gladieux and Chateau-Thierry have observed two apparently different components in convoy-electron velocity spectra and supposed that the width of one of the components is consistent with the theory of the WRC process,⁷ and (ii) Vager *et al.* have shown that projectile Rydberg atoms, formed during ion-solid interactions, are easily ionized by the electric field of the electron analyzer, and have discussed a possible contribution of the Rydberg ionization to the shape and intensity of the convoy-electron spec-

trum.⁸

In the present work, we have conducted an experiment to elucidate the *principal mechanisms for the convoy-electron production* in light-particle-solid interactions, with swift H^+ and H^0 (0.9–2.0 MeV/u) perpendicularly incident on carbon foils.

The details of the experimental apparatus used in the present work have been described previously.⁹ Therefore, only a brief description will be given below. The spectrometer used here is a 30° parallel-plate electrostatic analyzer, specially designed for measurements of secondary electrons produced by particle-solid interactions,¹⁰ having its object point on the projectile-target-foil interaction position and its image point on the exit slit of the spectrometer. This focusing condition enables one to use the wide entrance slit of the spectrometer, 5 mm in width, and thereby to observe electrons ejected in forward directions, reducing the background electrons produced by primary ions hitting the entrance slit to negligible levels. The energy resolution of the spectrometer is $\Delta E/E \sim 1.4\%$ (full width at half maximum), and the acceptance semiangles are 0.37° and 2.4° for the direction parallel and perpendicular to the rotation plane of the analyzer, respectively. A H^0 beam was produced by a carbon-foil neutralizer ($\sim 10 \mu\text{g}/\text{cm}^2$) followed by a pair of deflectors to remove charged components and also to let the metastable excited components decay by the Stark effect.

In Fig. 1, the electron spectra, $d^2n_e/dEd\Omega$, measured at 0° ($\pm 0.1^\circ$), 5°, 10°, 15°, and 30°, differential in electron energy E and ejection angle, multiplied by the electron energy E for 1.4-MeV/u H^0 incident on the 2.5- $\mu\text{g}/\text{cm}^2$ carbon foil are plotted as functions of electron energy. One can see that the observed convoy electrons consist of

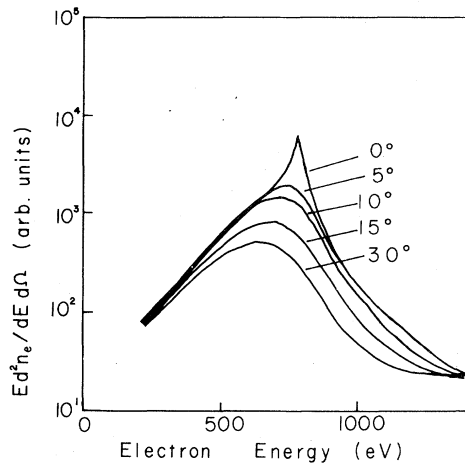


FIG. 1. Electron spectra, $E d^2 n_e / dE d\Omega$, differential in energy and ejection angle, multiplied by the electron energy E for 1.4-MeV/u H^0 on 2.5- $\mu\text{g}/\text{cm}^2$ carbon foil, observed at $0^\circ (\pm 0.1^\circ)$, 5° , 10° , 15° , and 30° .

two components, i.e., (i) a sharp cusp-shaped peak, which is observed only around 0° , and (ii) a broad peak or shoulder, whose intensity as well as peak energy slowly decreases with increasing angle. It was found that, for both H^0 and H^+ and for all the target thicknesses measured (1.5–60 $\mu\text{g}/\text{cm}^2$), the electron spectra observed at 0° are identical with those observed at small but nonzero ejection angles except for the narrow energy region around the cusp-shaped peak energy, within the experimental accuracy.

In Fig. 2 are shown the electron spectra, $E d^2 n_e / dE d\Omega$, measured at $0^\circ (\pm 0.1^\circ)$ for 2.0-MeV/u H^0 incident on 2.5-, 3.4-, and 5.2- $\mu\text{g}/\text{cm}^2$ carbon foils and for 2.0-MeV/u H^+ on a 60- $\mu\text{g}/\text{cm}^2$ carbon foil. Notice the following: (i) The peak height of the sharp cusp-shaped peak for H^0 rapidly decreases with increasing foil thickness, keeping the peak energy unaltered, and finally reaches that for the same-velocity H^+ (not shown in the figure). (ii) The intensity of the broad peak (shoulder) rapidly decreases and finally disappears with increasing foil thickness. This behavior of the broad peak is quite similar to that observed with H_2^+ , H_3^+ , and He^+ , where the origin of the broad peak was attributed to the ELC electrons suffering multiple collisions in the target foil.³ Accordingly, the broad peak and the sharp cusp-shaped peak will be referred to as the electron-loss convoy electrons (LCE) and the intrinsic convoy electrons (ICE), respectively.

In Fig. 3, the electron spectra, $E d^2 n_e / dE d\Omega$, measured at $0^\circ (\pm 0.1^\circ)$ for 2.0-MeV/u H^0 on 3.4 and 5.2 $\mu\text{g}/\text{cm}^2$ and H^+ on 60 $\mu\text{g}/\text{cm}^2$ and shown

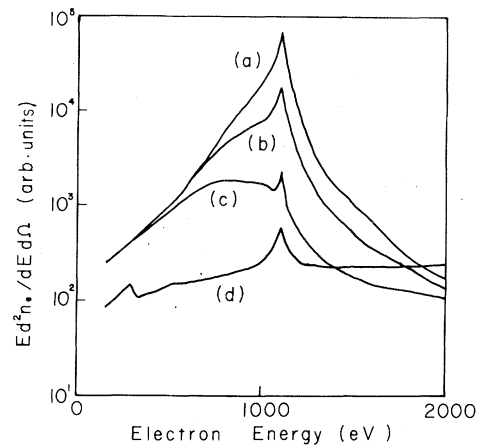


FIG. 2. Differential electron spectra, $E d^2 n_e / dE d\Omega$, at $0^\circ (\pm 0.1^\circ)$ for 2.0-MeV/u H^0 on (curve a) 2.5-, (curve b) 3.4-, and (curve c) 5.2- $\mu\text{g}/\text{cm}^2$ carbon foils and (curve d) for 2.0-MeV/u H^+ on a 60- $\mu\text{g}/\text{cm}^2$ carbon foil.

in Fig. 2 are replotted as functions of electron energy so that the peak heights of the spectra at the ICE peak energy are all normalized to 5. The dotted lines, separating the ICE parts from the other parts [hereafter referred to as background electrons (BGE)], refer to the spectra observed

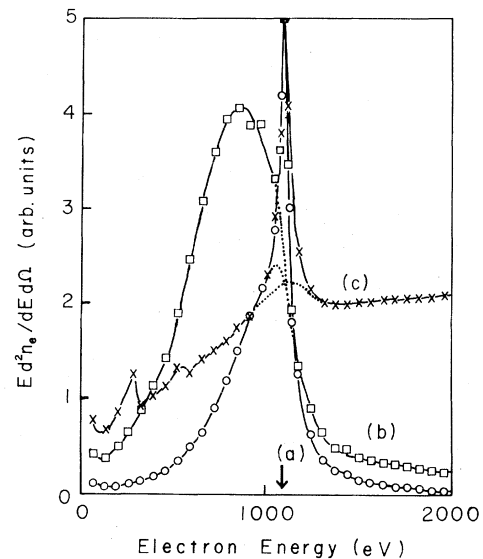


FIG. 3. Differential electron spectra, $E d^2 n_e / dE d\Omega$, at $0^\circ (\pm 0.1^\circ)$ for 2.0-MeV/u H^0 on (curve a) 3.4- and (curve b) 5.2- $\mu\text{g}/\text{cm}^2$ carbon foils and (curve c) for 2.0-MeV/u H^+ on a 60- $\mu\text{g}/\text{cm}^2$ carbon foil. The electron intensity is normalized to 5 at the ICE peak energy. The dotted lines refer to the spectra observed at a small but nonzero ejection angle ($\sim 5^\circ$). The arrow shows the peak energy of the ICE.

at a small but nonzero ejection angle ($\sim 5^\circ$). It should be noticed that all the dotted lines meet together at the ICE peak energy. The ICE peak height, I_{ICE} , and the ratio of the ICE peak height to the BGE intensity at the ICE peak energy, I_{ICE}/I_{BGE} , are plotted in Figs. 4(a) and 4(b), respectively, as functions of dwell times for 0.9-, 1.4-, and 2.0-MeV/u H^0 together with those for the same-velocity H^+ . The ratio, I_{ICE}/I_{BGE} , remains approximately constant for dwell times longer than ~ 0.8 fs (0.8×10^{-15} sec), whereas the ICE peak height varies by about two orders of magnitude. This observed linear proportionality between the ICE peak height and the BGE intensity at the ICE peak energy leads to the conclusion that the ICE strongly correlates with the BGE around the ICE peak energy. Further, taking account of the fact that the dominant production process of the BGE around the ICE peak energy changes from the ELC process to the target-electron ionization process as the foil thickness increases for incident H^0 or as the incident projectile is changed from H^0 to H^+ , it may be concluded that the ICE originate not from the previously proposed single-collision processes such as the TETC, the ELC, or the WRC,^{11,12} but instead from some final-state interaction between the projectile ion and the BGE which are produced in the target foil and escape from the exit surface of the target after some collisions with target atoms. In other words, the ICE may be produced by the free electron transfer to the projectile continuum (FETC) process. It is possible that the surface potential at the exit surface of the target may play some role in this transfer process. In heavy-ion-solid interactions, a similar mechanism has been proposed by Betz, Rosenthaler, and Rothermel¹³ for Rydberg formation, i.e., they have discussed a possible significance of the ELC electrons undergoing a transition back to Rydberg states of the projectile upon emergence from the target foil. In Fig. 4(b), the increase of the ratio, I_{ICE}/I_{BGE} , for shorter dwell times $\lesssim 0.8$ fs may reflect the fact that the direct ELC process dominates over the FETC process in this dwell-time region.

According to the above discussion, the ICE spectrum, $d^2n_{ICE}/dEd\Omega$, may be tentatively ex-

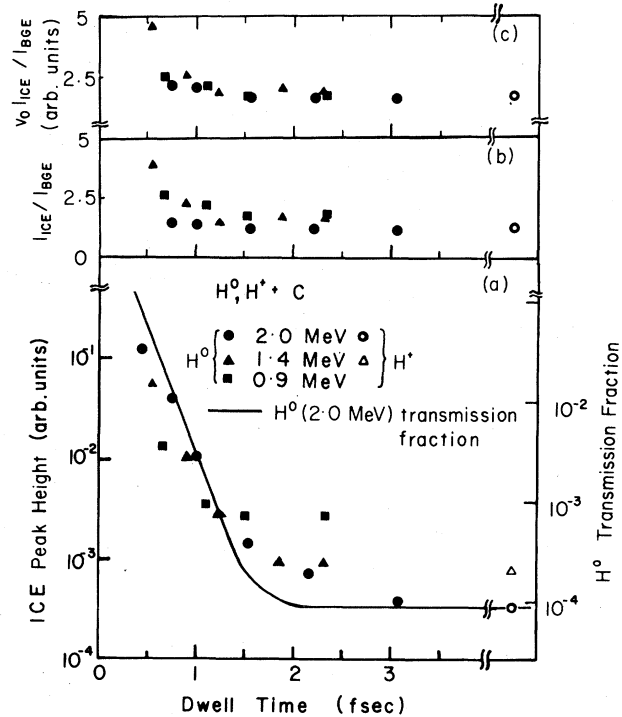


FIG. 4. (a) The ICE peak height, I_{ICE} , together with the transmission fraction for 2.0-MeV/u H^0 (Naitoh *et al.*, Ref. 14); (b) the ratio of the ICE peak height to the BGE intensity at the ICE peak energy, I_{ICE}/I_{BGE} ; and (c) the modified ratio, $v_0 I_{ICE}/I_{BGE}$, as functions of dwell time.

pressed by

$$\frac{d^2n_{ICE}}{dE d\Omega} = |\vec{v} - \vec{v}_0|^{-1} \alpha(\vec{v}, \vec{v}_0) \frac{d^2n_{BGE}}{dE d\Omega}, \quad (1)$$

where \vec{v} is the electron velocity, \vec{v}_0 the projectile velocity, $|\vec{v} - \vec{v}_0|^{-1}$ a factor from the projectile-centered Coulomb wave function describing the final states,⁶ $\alpha(\vec{v}, \vec{v}_0)$ a slowly varying function of \vec{v} and \vec{v}_0 , which couples the ICE intensity with the BGE intensity, and $d^2n_{BGE}/dE d\Omega$ the differential BGE spectrum. The observed ICE energy spectrum, $\langle d^2n_{ICE}/dE d\Omega \rangle$, is derived by integrating Eq. (1) over the acceptance solid angle of the analyzer. Under a reasonable assumption that the $d^2n_{BGE}/dE d\Omega$ is a slowly varying function of \vec{v} , the ICE spectrum at 0° is written, for the electron analyzer with a round aperture of acceptance semiangle θ_0 ,

$$\left\langle \frac{d^2n_{ICE}}{dE d\Omega} \right\rangle_{0^\circ} = \frac{2\pi}{vv_0} [(v^2 + v_0^2 - 2vv_0 \cos\theta_0)^{1/2} - |v - v_0|] \alpha(\vec{v}, \vec{v}_0) \Big|_{0^\circ} \frac{d^2n_{BGE}}{dE d\Omega} \Big|_{0^\circ}. \quad (2)$$

The ICE peak height ($v = v_0$) at 0° is then written,

$$\left\langle \frac{d^2 n_{ICE}}{dE d\Omega} \right\rangle_{0^\circ, v=v_0} = \frac{4\pi \sin(\theta_0/2)}{v_0} \alpha(\vec{v}, \vec{v}_0) \Big|_{0^\circ, v=v_0} \frac{d^2 n_{BGE}}{dE d\Omega} \Big|_{0^\circ, v=v_0}. \quad (3)$$

Equation (3) shows that the ratio,

$$\langle d^2 n_{ICE}/dE d\Omega \rangle_{0^\circ, v=v_0} / \langle d^2 n_{BGE}/dE d\Omega \rangle_{0^\circ, v=v_0}$$

is inversely proportional to the projectile speed v_0 as long as the factor $\alpha(\vec{v}, \vec{v}_0)$ remains constant. Accordingly, the ratio, I_{ICE}/I_{BGE} , shown in Fig. 4(b), equivalent to the ratio

$$\langle d^2 n_{ICE}/dE d\Omega \rangle_{0^\circ, v=v_0} / \langle d^2 n_{BGE}/dE d\Omega \rangle_{0^\circ, v=v_0},$$

is replotted by multiplying the projectile speed v_0 in Fig. 4(c). Figure 4(c) shows that the modified ratio, $v_0 I_{ICE}/I_{BGE}$, is approximately independent of the projectile energy, as Eq. (3) predicts.

Finally, let us compare the ICE peak height with the H^0 transmission fraction¹⁴ as functions of the dwell time, for 2.0-MeV/u incident H^0 , in Fig. 4(a). The fact that both quantities show a remarkable similarity in their gross behaviors as seen in Fig. 4(a) may provide new information for the mechanisms of neutral formation in swift-ion-solid interactions, although the details need further investigation.

¹For a recent review, see I. A. Sellin, in *Physics of Electronic and Atomic Collisions*, edited by S. Datz (North-Holland, Amsterdam, 1982), p. 195; V. H. Ponce, E. Gonzalez Lepera, W. Meckbach, and I. B. Nemirovsky, *Phys. Rev. Lett.* **47**, 572 (1981), and references therein.

²K. Dettmann, K. G. Harrison, and M. W. Lucas, *J. Phys. B* **7**, 269 (1974).

³R. Latz *et al.*, *IEEE Trans. Nucl. Sci.* **30**, 913 (1983); N. Oda, Y. Yamazaki, and Y. Yamaguchi, Oak Ridge National Laboratory Report No. CONF-820131, 1983 (unpublished), p. 256.

⁴V. N. Neelavathi, R. H. Ritchie, and W. Brandt, *Phys. Rev. Lett.* **33**, 302 (1974).

⁵In ion-solid-foil collisions, observed electron spectra do not depend on the foil thickness for foils sufficiently thicker than the mean free path of the electron in question. Accordingly, such spectra will be termed "equilibrium spectra" hereafter.

⁶W. Steckelmacher, R. Strong, M. N. Khan, and M. W. Lucas, *J. Phys. B* **11**, 2711 (1978); W. Meckbach, N. Arista, and W. Brandt, *Phys. Lett.* **65A**, 113 (1978).

⁷A. Gladioux and A. Chateau-Thierry, *Phys. Rev. Lett.* **47**, 786 (1981).

⁸Z. Vager *et al.*, *Phys. Rev. Lett.* **48**, 592 (1982).

⁹N. Oda, F. Nishimura, Y. Yamazaki, and S. Tsurubuchi, *Nucl. Instrum. Methods* **170**, 571 (1980); Y. Yamazaki and N. Oda, *Nucl. Instrum. Methods* **194**, 323 (1982).

¹⁰Y. Yamazaki, N. Oda, and A. Yasaka, to be published.

¹¹Our statement does not exclude the possibility that some fraction of the secondary electrons traveling with velocity $\vec{v} \sim \vec{v}_0$ in the target foil are influenced by the wake potential.

¹²Z. Vager *et al.*, *Phys. Rev. Lett.* **50**, 1017 (1983), reported that the field-ionized electrons from the Rydberg atoms were about 10% of the total convoy electrons and were shifted upwards by about 18 eV. Taking into account these findings and that the electric field applied to our electron analyzer (30° deflection) is weaker than that applied to Vager *et al.*'s (45° deflection), we expect the field-ionized electrons with the ICE peak energy to give only a minor contribution to the ICE peak height.

¹³H. D. Betz, D. Rosenthaler, and J. Rothermel, *Phys. Rev. Lett.* **50**, 34 (1983).

¹⁴M. J. Gaillard *et al.*, *Phys. Rev. A* **16**, 2323 (1977); H. Naitoh, T. Yonenaga, T. Ichimori, and N. Oda, in "Atomic Collision Research in Japan No. 8, 1982" (unpublished), p. 303.